LONDON, METEOROLOGICAL OFFICE.

Met.O. 19 Branch Memorandum No. 25.

Satellite retrievals of thickness: a statistical method for predicting retrieval error and its application to the optimal positioning of SSU weighting functions. By COOK, I.S.

London, Met.Off., Met.O.19 Branch Mem.No.25, 1975, 1975, 31cm.Pp.[20].1 Ref.

An unofficial document - restriction on first page to be observed.

LBN

MET O 19 BRANCH MEMORANDUM NUMBER 25

SATELLITE RETRIEVALS OF THICKNESS: A STATISTICAL METHOD FOR PREDICTING RETRIEVAL ERROR AND ITS APPLICATION TO THE OPTIMAL POSITIONING OF SSU WEIGHTING FUNCTIONS.

I S COOK

LBN

SATELLITE RETRIEVALS OF THICKNESS: A STATISTICAL METHOD FOR PREDICTING RETRIEVAL ERROR AND ITS APPLICATION TO THE OPTIMAL POSITIONING OF S.S.U. WEIGHTING FUNCTIONS

I.S. COOK

Introduction

This memorandum is in two parts. The first of these is concerned with the prediction of thickness retrieval error using a sample of rocketsonde temperature profiles. It is assumed that thickness would be retrieved from a set of measured radiances via a linear regression equation with suitable coefficients. Now, the major source of retrieval error lies in the ambiguity of the information received by the radiometer, i.e., in the range of possible thickness values consistent with a given set of radiances. By expressing thickness in terms of equivalent radiance and computing, for every profile in the sample, (a) the equivalent radiance and (b) a set of simulated "measured" radiances, a covariance matrix of both (a) and (b) radiances can be constructed. After a simple correction for instrumental noise, the inverse form of this matrix will yield values for the set of linear regression coefficients and for the standard error of estimate of equivalent radiance. From the latter, a representative value for the SEE of thickness can be derived.

Part II of the memorandum is concerned with the application of this method to a specific problem, viz: whether an adjustment to the planned separations of the SSU weighting functions would lead to a reduction in the expected retrieval errors of pressure surface contour heights. It was assumed that these contours would be obtained by adding retrieved thicknesses to conventionally derived low-level contours. As regards the positioning of weighting functions, there is a danger that different criteria of optimisation could lead to different conclusions, and the choice of any particular criterion is bound to be somewhat arbitrary. Nevertheless, the criterion used in the investigation was felt to be sufficiently close to real conditions for the conclusions drawn to carry some weight.

PART I: DERIVATION OF THE STANDARD ERROR OF ESTIMATE OF RETRIEVED THICKNESS

Sources of retrieval error

The linear regression equation relating the most probable value of an atmospheric thickness to a set of satellite radiometer measurements is:

$$f(\Theta)_{est.} - f(\overline{\Theta}) = \sum_{i=1,n} A_i (R_i - \overline{R}_i) \qquad (1)$$

where Θ = thickness

$f(\Theta)$ = an equivalent radiance representing Θ, and a unique function of Θ

n = number of radiometer channels

R_i = the ith measured radiance

A_i = the ith regression coefficient

Bars denote mean values from a statistical sample representing the population to which the hypothetical sounding above belongs. (The population might include soundings made over the entire atmosphere, but is more likely to be confined to a certain latitude band and season). The sample is also used to compute the regression coefficients, the criterion being that, given R_i ..... R_n, the estimate for $f(\Theta)$ is the most probable value.

The difference between the "retrieved" estimate of $f(\Theta)$ and its actual value (in the atmosphere) is the retrieval error. The main sources of retrieval error are as follows:

(a) Owing, for example, to inadequate size, or to the injudicious selection of profiles in it, the sample chosen to represent a given population is not accurately representative, so that the regression coefficients are in error. Alternatively, the chosen population may itself be too heterogeneous for a single set of regression coefficients to suffice. Although this problem has yet to be investigated in detail, the coefficients are not in fact thought to be critically dependent on latitude and season, so that this source of retrieval error is not regarded as a serious limitation.

(b) The actual relation between $f(\Theta)$ and the radiances contains a degree of non-linearity, so that a complete description of it would require cross-product and squared terms, etc. In practice however, if a population is confined to a limited range of latitude, and to a particular season, the deviation from mean conditions is small enough for the linear approximation to remain valid for a majority of soundings.

(c) Each of the radiance values processed by the instrument is susceptible to random noise of known variance.

(d) The estimate of $f(\Theta)$ derived from equation 1 (above) represents the most probable value, i.e. the value for which the probability function (of $f(\Theta)$ given the radiances) is a maximum. Centred on this maximum probability value is a range of less probable values, giving rise to an error of estimate that represents the most important source of retrieval error. The measurements made by the radiometer thus contain an inherent ambiguity as regards interpretation in terms of $f(\Theta)$. This ambiguity is a limitation of satellite sounding systems which cannot be bypassed. The standard error of estimate (SEE) for $f(\Theta)$, which (as shown below) can be computed from a sample of profiles, represents the limit of accuracy with which $f(\Theta)$ can be retrieved using a satellite radiometer.

When instrumental noise (see (c) above) is also taken into account, the SEE for $f(\Theta)$ is a useful criterion for judging the expected overall performance of a radiometer generally, and (more specifically) for optimising instrumental parameters such as the position of weighting function peaks (see part II).

Deviation of the SEE of thickness from a sample of temperature profiles

Consider a large sample of (rocketsonde) temperature profiles from a distinct latitude band and season. From each profile is derived, using appropriate weighting functions, the set of n radiances which would be measured by a satellite radiometer directly overhead, instrumental noise being ignored for the time being. Also derived in each case is the thickness of a given atmospheric slab. In order to reduce the non-linearity in the relationship between radiances and thickness, the thickness is expressed in terms of the Planck function of mean slab temperature (PFMST). The PFMST is a unique function of thickness, has dimensions of radiance, and from this stage is treated as a supplementary $(n + 1)$th radiance R_*. The sample as a whole is now used to construct a radiance covariance matrix of order $(n + 1)$ by $(n + 1)$.

Now the estimate of the covariance C_{ij} between radiances i and j is given by:

$$C_{ij} = C_{ji} = \frac{1}{S - 1} \sum_{s=1,\ S} (R_{is} - \overline{R}_i)(R_{js} - \overline{R}_j) \qquad (2)$$

where S = number of profiles in sample

R_{is} = the ith radiance in the sth profile

$\overline{R}$ = sample mean of ith radiances

At this point, the correction for instrumental noise is made by adding an $(n + 1)$ by $(n + 1)$ noise covariance matrix to the radiance covariance matrix. Now the noise components of different channels are uncorrelated (because the noise is random), so that the noise covariance matrix is diagonal and consists only of the noise variances for each channel. Thus the noise correction leaves unaffected all the inter-channel radiance covariances, and modifies only the radiance variances. It should be noted that only the simulated satellite radiances are susceptible to instrumental noise; the noise corresponding to the PFMST "channel" is zero, and the variance of R_* is unchanged by the correction.

The noisy-radiance covariance matrix, which is of order $(n + 1)$ by $(n + 1)$, thus contains the covariances of the n noisy radiances and the supplementary R_*.

For the sake of clarity, n will be given the value three from this stage.

Consider now a satellite radiometer sounding a temperature profile which belongs to the same population as the sample used to derive the noisy-radiance covariance matrix. The output of the radiometer consists of a set of three noisy-radiances, R_1 R_2 and R_3. The maximum probability estimate of R_* for the profile is found, together with the standard error of estimate, as follows:

$$\text{Firstly, let } \left.\begin{aligned} r_1 &= R_1 - \overline{R}_1 \\ r_2 &= R_2 - \overline{R}_2 \\ r_3 &= R_3 - \overline{R}_3 \\ R_* &= R_* - \overline{R}_* \end{aligned}\right\} \text{ where } \overline{R}_1\ \overline{R}_2\ \overline{R}_3 \text{ and } \overline{R}_* \text{ are sample means}$$

Now, the probability density function $P(r_1\ r_2\ r_3\ r_*)$ for $r_1\ r_2\ r_3$ and r_* as variables is given by:

$$-2 \log_e P(r_1\ r_2\ r_3\ r_*) = \begin{bmatrix} r_1 & r_2 & r_3 & r_* \end{bmatrix} \begin{bmatrix} \text{INVERSE} \\ \text{NOISY-} \\ \text{RADIANCE} \\ \text{COVARIANCE} \\ \text{MATRIX} \end{bmatrix} \begin{bmatrix} r_1 \\ r_2 \\ r_3 \\ r_* \end{bmatrix} + \text{constant} \qquad (3a)$$

Let the inverse noisy-radiance covariance matrix be denoted by $\underline{K}$, so that K_{ij} is the element in row i and column j. $\underline{K}$ is symmetrical, so that $K_{ij} = K_{ji}$.

$$-2 \log_e P(r_1\ r_2\ r_3\ r_*) = \begin{bmatrix} r_1 & r_2 & r_3 & r_* \end{bmatrix} \begin{bmatrix} K_{11} & K_{21} & K_{31} & K_{41} \\ K_{21} & K_{22} & K_{32} & K_{42} \\ K_{31} & K_{32} & K_{33} & K_{43} \\ K_{41} & K_{42} & K_{43} & K_{44} \end{bmatrix} \begin{bmatrix} r_1 \\ r_2 \\ r_3 \\ r_* \end{bmatrix} + \text{constant} \qquad (3b)$$

If the given values of r_1 r_2 and r_3 are substituted into $P(r_1\ r_2\ r_3\ r_*)$, an expression for $P(r_*/r_1\ r_2\ r_3)$, the probability density of r_* given r_1 r_2 and r_3, can be found from Bayes' theorem:

$$P(r_* \mid r_1\ r_2\ r_3) = P(r_1\ r_2\ r_3\ r_*)/P(r_1\ r_2\ r_3)$$

$$\therefore \log_e P(r_*/r_1\ r_2\ r_3) = \log_e(r_1\ r_2\ r_3\ r_*) + \text{constant } (r_* \text{ is the only variable})$$

so that: $$-2 \log_e P(r_*/r_1\ r_2\ r_3) = \begin{bmatrix} r_1 & r_2 & r_3 & r_* \end{bmatrix} \begin{bmatrix} K_{11} & K_{21} & K_{31} & K_{41} \\ K_{21} & K_{22} & K_{32} & K_{42} \\ K_{31} & K_{32} & K_{33} & K_{43} \\ K_{41} & K_{42} & K_{43} & K_{44} \end{bmatrix} \begin{bmatrix} r_1 \\ r_2 \\ r_3 \\ r_* \end{bmatrix} + \text{constant} \qquad (3c)$$

when the given values of r_1 r_2 and r_3 are substituted.

Multiplying out eqn.3c, and incorporating all terms not involving r_* into the "constant", gives the variation of $P(r_*/r_1\, r_2\, r_3)$ with r:

$$-2\log_e P(r_* | r_1\, r_2\, r_3) = K_{44} r_*^2 + 2(K_{41} r_1 + K_{42} r_2 + K_{43} r_3) r_* + \text{const.} \quad (4)$$

Compare equation 4 with the equation for a (one-dimensional) Gaussian distribution of a function x with standard deviation σ centred at x_0:

$$-2\log_e P(x - x_0) = \frac{x^2}{\sigma^2} - \frac{2x_0 x}{\sigma^2} + \text{constant} \quad (5)$$

Clearly, equation 4 represents a Gaussian distribution of standard deviation $1/\sqrt{K_{44}}$ centred at:

$$r_* = -\frac{K_{41}}{K_{44}} r_1 - \frac{K_{42}}{K_{44}} r_2 - \frac{K_{43}}{K_{44}} r_3 \quad (6)$$

Compare equation 6 with equation 1. The linear regression coefficients for the maximum probability estimate of r_* are given by:

$$A_i = -\frac{K_{4i}}{K_{44}} \quad \text{where } i = 1, 4 \quad (7a)$$

The standard deviation of the distribution (in equation 4) is the standard error of estimate for r_*. It is independent of the actual values of r_1, r_2, and r_3, and can thus be derived from the noisy-radiance covariance matrix (as can the regression coefficients).

This method can easily be generalised to the case of an n channel radiometer. Writing m = n + 1, the regression coefficient for the ith radiance will be:

$$A_i = -K_{mi}/K_{mm} \quad (7b)$$

and the SEE of r_* will be:

$$\text{SEE} = 1/\sqrt{K_{mm}} \quad (8)$$

It should be noted that although r_* has the same dimensions as r_1, r_2, and r_3, the method described above for determining its SEE does not require that this be the case. A dimensionless form of equation 3 exists with the inverse noisy-radiance correlation matrix (instead of the covariance matrix), and statistical t-values of the radiances (instead of the radiances themselves).

For a detailed description of the application of probability theory to satellite sounding techniques, see Rodgers (1969).

For practical purposes, it is helpful to represent the standard error of estimate in terms of actual thickness retrieval error in decametres. This is the best criterion for deciding whether, for instance, a realistic high-level pressure surface contour height can be obtained by adding a retrieved thickness to a known low-level contour. In addition, even with the SEE of mean slab temperature constant, the SEE of thickness increases proportionately with slab depth, and this dependence is an important limitation as regards the retrieval of very "deep" slabs (see equation 10a).

The thickness Θ, in dm, of an atmospheric slab of depth n levels (on the Oxford pressure level system) is given by:

$$\Theta = 0.586026.\ n.\ T \tag{9}$$

where T is the mean slab temperature, in K.

Thus, the SEE of thickness, $\delta\Theta$, is related to a corresponding error in mean temperature δT by:

$$\delta\Theta = 0.586026\,\Delta n\,\delta T \tag{10a}$$

In terms of the SEE of the PFMST, δR_*, this becomes:

$$= 0.586026\,\Delta n \left(\frac{\partial T}{\partial R_*}\right)_{R'_*} \delta R_* \tag{10b}$$

where R'_* is the maximum probability estimate of R_*

Thus there is in fact no single value of $\delta\Theta$ corresponding to a given value of δR_* because of the dependence on $\partial T/\partial R_*$, but a representative value for Θ can be derived by setting $\partial T/\partial R_*$ to its sample mean. Now, to a close approximation:

$$\overline{\left(\frac{\partial T}{\partial R_*}\right)} \simeq \left(\frac{\partial T}{\partial R_*}\right)_{\overline{R}_*} \tag{11}$$

where $\overline{R}_*$ is the sample mean

which gives:

$$\delta\Theta \simeq 0.586026.\Delta n.\left(\frac{\partial T}{\partial R_*}\right)_{\overline{R}_*}.\ \delta R_* \tag{10c}$$

PART II: OPTIMISATION OF THE POSITIONS OF THE SSU CHANNELS

Introduction

When the Tiros N Stratospheric Sounder Unit (SSU) becomes operational, one possible use for it will be the provision of thickness retrievals of atmospheric slabs with lower surfaces in the lower stratosphere (50 mb was the pressure level used in the initial analysis) and upper surfaces in the region from 20 mb to 1 mb. From this information, contour heights of high-level pressure surfaces can be found by adding the retrieved thickness to low-level contours obtained by conventional means.

A statistical method was described in part I, which, when given a set of radiometer weighting functions, can predict for any atmospheric slab the standard error of estimate (SEE) of retrieved thickness. If this is done for a series of slabs with fixed lower surface and variable upper surface, then, provided that errors in the low-level contour are assumed small in comparison with the retrieval errors, the SEE of slab thickness can be identified with the SEE of contour height, and a profile of contour height SEE values obtained.

It is proposed to use the shape of the atmospheric profile of contour height SEE (as defined above) as a criterion for optimising the positions of the SSU weighting functions.

It was assumed throughout the investigation that additional radiances from the top two BSU (Basic Sounder Unit) channels, (labelled 'D' and 'E') would be available. Neither of these is affected by the presence of high cloud, but peaking as they do at about 40 mb and 60 mb respectively, both provide additional information in the regions of interest.

The SSU channels, here labelled 'A', 'B', and 'C', peak at around 1.5 mb, 4 mb, and 15 mb respectively.

The analyses were initially carried out using a sample of 75 temperature profiles (derived from rocket sondes) belonging to the Winter 50-70 deg population. This population represents a "worst case" because of its variability. As a check, a second set of analyses was carried out using a sample from the tropics.

Results: Initial Analyses (50 mb)

Fig 1 shows for the winter 50-70 and tropical samples the effect on the (nominal) contour height SEE profile of excluding each SSU channel in turn. The continuous curve represents the contour height SEE profile derived from the five nominal channels (radiances from the two BSU channels have been included in every derivation). The absolute SEE has a dependence on slab depth (see equ 10c), so that it tends towards zero as the pressure surface tends towards level 16.

In terms of the effect on the nominal profile of its exclusion, channel C would appear to make the most important contribution in the region of interest (20mb to 1mb). The largest discrepancy occurs at around level 28.

Below level 36, the exclusion of channel A has negligible effect on the contour height SEE values. The choice of 50mb as the common atmospheric slab base, and the limiting of the investigation to levels below 40 has effectively excluded the areas where channel A would be expected to make its main contribution to thickness retrievals.

In Fig 2, the SSU weighting functions have been "shifted" up and down in order to determine the effect on the nominal profile of changes in the separation between adjacent weighting function peaks. The function plotted against contour height in each of these diagrams is the deterioration (increase) in SEE relative to the nominal profile (continuous curves in Fig 1). See the appendix for details of the "shifting" technique, and for the derivation of instrumental noise variances for the various weighting functions.

The two temperature profile samples (winter 50-70 deg, and tropical) are highly dissimilar. The tropical sample analyses were carried out in order to check that the qualitative effects of the weighting function shifts were not over-influenced by the choice of sample. In fact, a satisfactory degree of consistency between the two samples is apparent in the results from fig 2.*

In general, the best correlation of a slab thickness (in terms of equivalent radiance) with a given radiance occurs when its geometric mean pressure coincides with the "centre of gravity" of the weighting function. In the case of channel C, which peaks at approximately 15mb, upper surfaces at about 4.5mb will be favoured (with lower surface at 50mb), and this is why the exclusion of channel C has such a pronounced effect on the SEE at about this level. This principle also applies when the radiance in question is actually a weighted mean of several real radiances, as is the case when a series of measured radiances is combined in a linear regression equation. Slabs other than those with maximum correlation with one of the "real" radiances will usually correlate well with an interpolated radiance of this kind, provided that there is a good degree of overlap between adjacent weighting functions. Optimisation of channel positions for a range of slabs depends on a compromise (which need not be particularly severe) between two conflicting requirements as follows:

1. the weighting functions must be sufficiently widely spaced to cover the required range.

* The uncertainty in the predicted SEE due to the use of a finite sample (75 profiles) is about an order of magnitude less than the SEE itself.

2. the weighting functions must overlap sufficiently for interpolated radiances to correlate well with their corresponding slabs.

It is unlikely that slabs with GM pressure of less than about 2mb (eg the 10-0.5mb thickness) will be retrieved. As far as thickness retrievals are concerned then, the highest weighting function need not peak higher than level 32 (channel A in fact peaks at level $33\frac{1}{2}$). With the highest BSU channel peaking at about level 18, the separation between the SSU channels ought not to be less than 4-5 levels. The object of the graphs in Fig 2 is to determine, for each of the three "gaps" C/BSU, B/C and A/B, the optimum separation between the weighting function peaks when this limitation is taken into account. Since the BSU channels are fixed, this effectively determines the optimum positions of the SSU channels.

As each gap is adjusted, so the other gaps are maintained at their nominal values. For example, as the gap between the weighting function peaks of channels B and C is given values of +4, +2, -2 and -4 levels relative to the nominal separation of $6\frac{1}{2}$ levels, so the separations between (1) channel C and the BSU channels, and (2) channels A and B are held constant. Effectively this means that while channel C, and the BSU channels, are fixed, channels A and B are moved up and down together, and the optimum separation between channels B and C can be determined from observed changes in the contour height SEE profile. A similar argument applies to the other gaps.

It is clear from Fig 2a that a reduction of 2 levels in the separation between channel C and the BSU channels, leads to an imporvement in the SEE profile at around level 23 of 0.6dm, at the expense of a deterioration of similar magnitude at higher levels. (This pattern is also apparent, though not so pronounced, in the tropical profile of Fig 2b). The nominal separation appears to be quite satisfactory; none of the other curves shows an overall improvement upon it. The +2 curve shows a serious deterioration of 2.4dm (max), and is unsatisfactory. Note that, since channel A (together with channel B) is being shifted up and down with channel C, there are changes in the coverage above the channel A peak which affect the SEE profile at levels beyond the regions of interest.

Fig 2c shows that a reduction of 2 levels in the separation between channels B and C leads to a slight overall improvement of 0.3dm (max). The nominal separation again appears to be quite satisfactory (relative to the best that can be achieved), and only the +4 curve shows a prominent deterioration. This result is qualitatively confirmed by Fig 2d (tropical).

Fig 1 showed that the exclusion of channel A has almost no effect at all on the controu height SEE profile below about level 36 (0.9mb). Hence it is not surprising that changes in the separation between channels A and B have very little influence below this level.

Results with a 10mb base

Fig 3 shows the contour height SEE profiles (as defined in the introduction) with the lower surfaces of the atmospheric slabs at level 24 (10.2mb). The SEE between 5mb and 2mb is actually greater than the corresponding errors for bases at 50mb (Fig 1) and 100mb (Fig 5). However, for the 1mb pressure surface, there is a clear advantage in the use of 10mb as the slab base (lower surface). The exclusion of channel B now makes the greatest impact on the overall SEE, with channel C of comparitively minor importance. Surprisingly, the exclusion of channel A is once again of significance only above level 36.

Fig 4a shows that an improvement of 1.4dm (max) can be obtained by spacing channels B and C closer together. At the levels where the 10mb base "comes into its own" (approximately between levels 35 and 39), the advantage of the -2 curve is slight. The +2 curve shows a serious deterioration at all levels below 40, so that the nominal spacing between the two channels must be regarded as a maximum.

Fig 4c shows that a slight improvement between levels 35 and 39 could be obtained by spacing channels A and B closer together; this would be at the expense of a rapid tail off above level 39 due to lack of coverage above the topmost channel.

Results with a 100mb base

Fig 5 shows the contour height SEE profiles with the lower surfaces of the atmospheric slabs at level 12.5 (101.6mb). The results are broadly similar to those in Fig 1 (50mb base) although, surprisingly, retrievals in the 10mb to 2mb region are slightly improved. An analysis along similar lines to that displayed in Fig 2 yielded very similar results.

Conclusion

If the retrieval of contour heights (as defined in the introduction) between 20mb and 1mb is accepted as a suitable criterion, then the following conclusions can be drawn:

Channel A in its nominal position makes almost no contribution to retreivals below level 36 (0.9mb). It might be more useful if it were lowered by 2-4 levels, though improvements gained would be at the expense of retrievals in the region 0.5mb to 1.0mb.

The nominal separations between (1) channel C and the BSU channels, and (2) channels B and C, are satisfactory, but should not be increased. Some improvement could be gained by lowering channel B by around 2 levels.

Fig 7 shows the changes in the SEE profile (relative to the nominal profiles) which occur when channel A is lowered by 3 levels and channel B by 2 levels. The resulting profiles should be close to the best that can be achieved, but they still represent only a slight improvement*(mostly less than 0.5dm) on the nominal profiles.

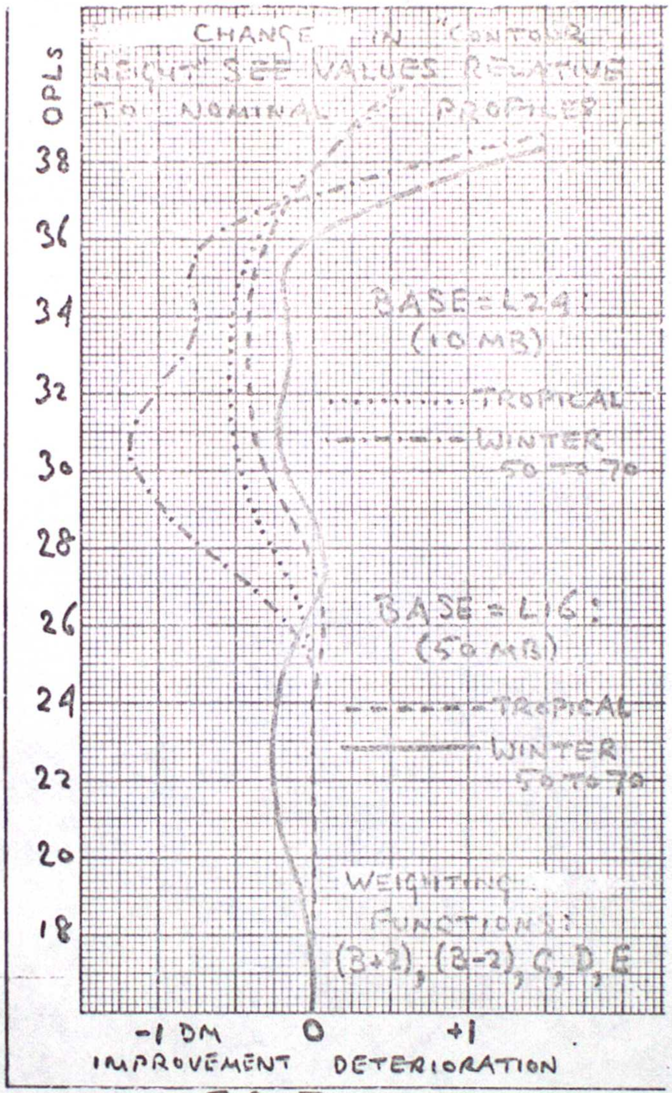

FIG 7

Reference

C D Rodgers: "Remote Sounding of the Atmospheric Temperature Profile in the Presence of Cloud"
Clarendon Lab. Memo No 69. 3. December 1969

* with the exception of slabs around 10-3 mb, which show a more substantial improvement of 1.4 dm (max).

STANDARD ERROR OF ESTIMATE OF CONTOUR HEIGHT (SEE TEXT) AS A FUNCTION OF PRESSURE LEVEL: SEQUENTIAL EXCLUSION OF SSU CHANNELS - WINTER 50 TO 70

BASE = 50 MB

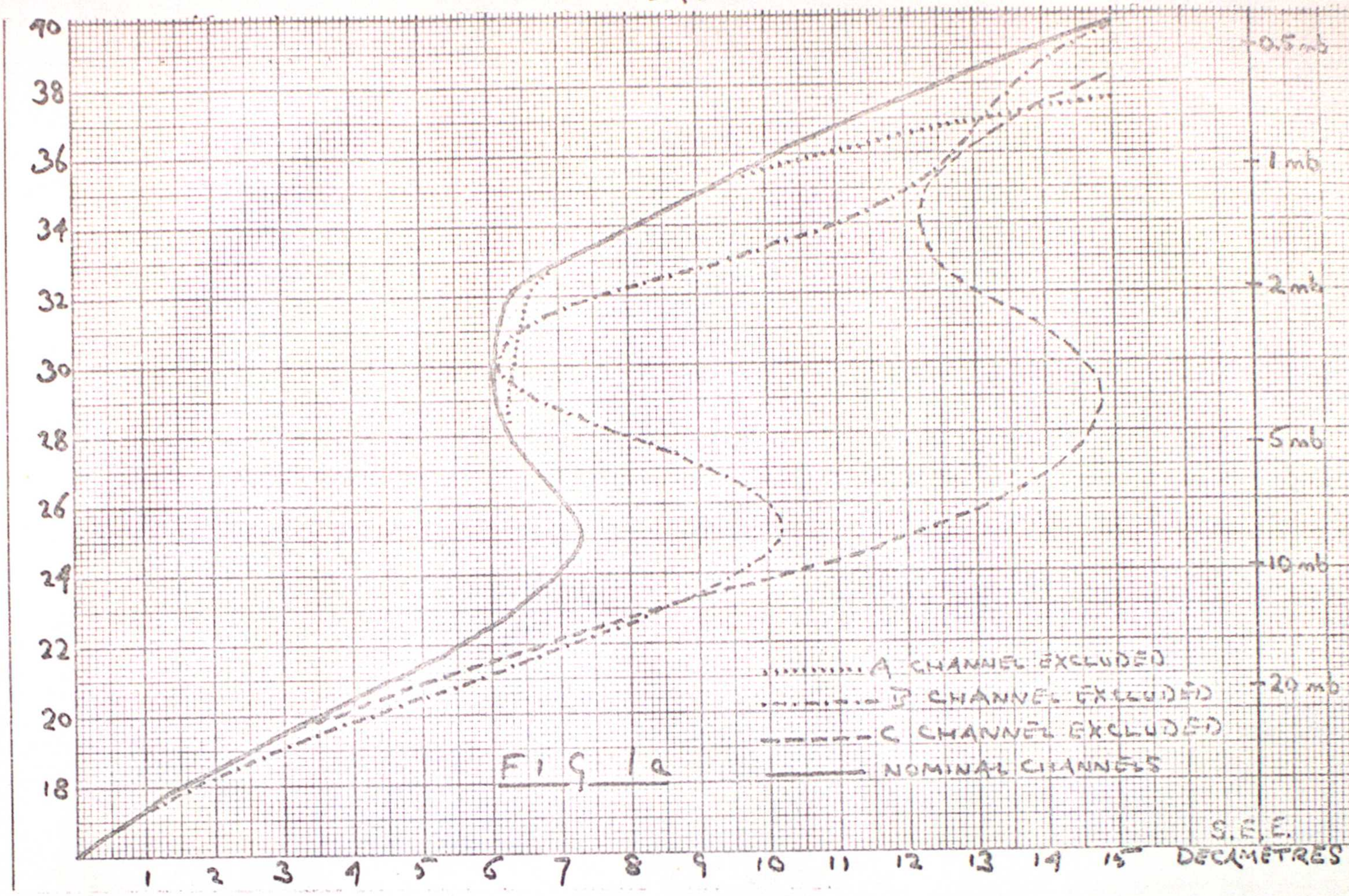

STANDARD ERROR OF ESTIMATE OF CONTOUR HEIGHT (SEE TEXT) AS A FUNCTION OF PRESSURE LEVEL: SEQUENTIAL EXCLUSION OF SSU CHANNELS - TROPICAL

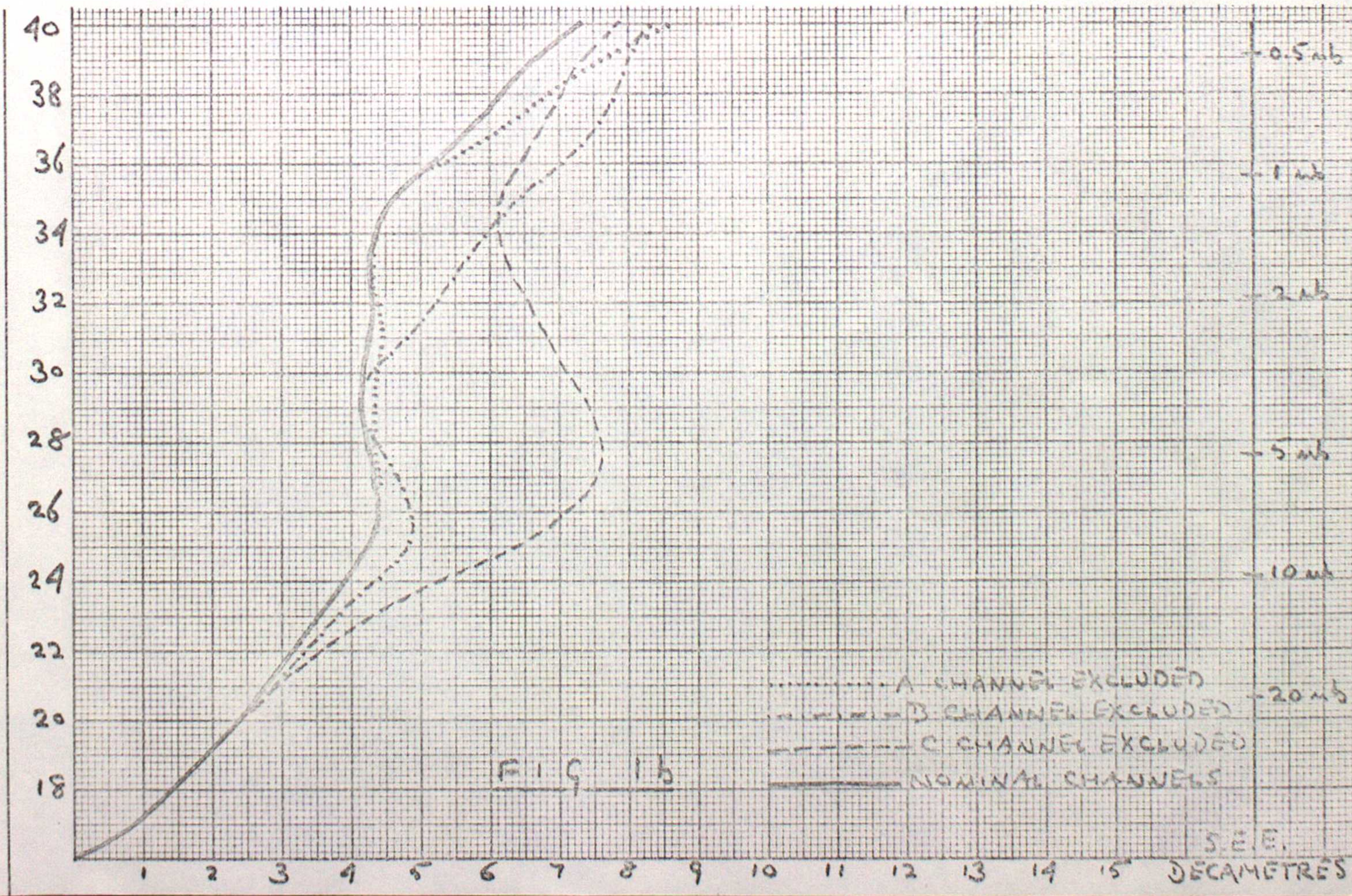

DETERIORATION IN "CONTOUR HEIGHT" SEE VALUES AS EACH INTER-CHANNEL SEPARATION IN TURN IS ALTERED. BASE = 50 MB

FIG 2A

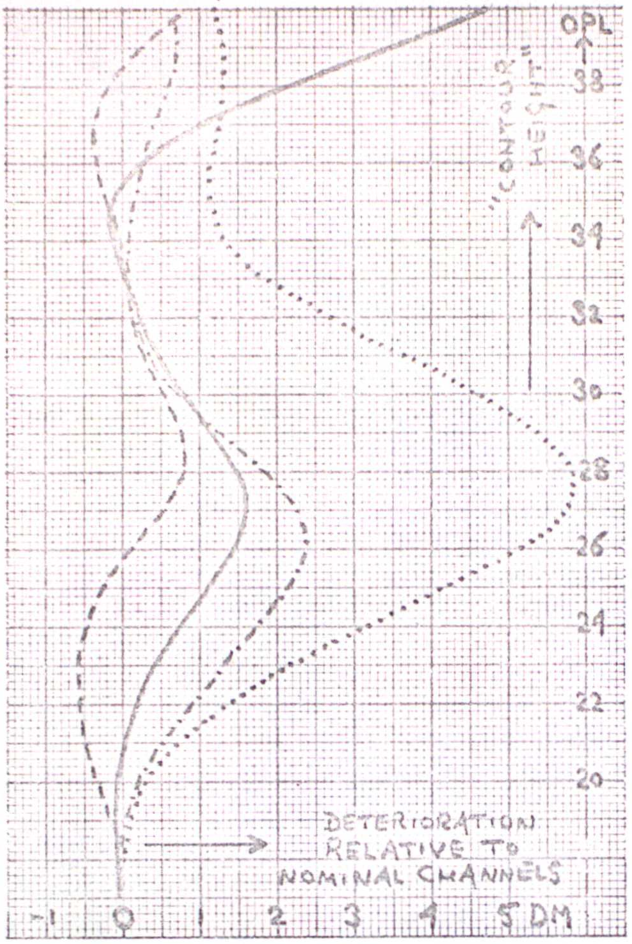

GAP C/BSU WINTER 50 TO 70

FIG 2B

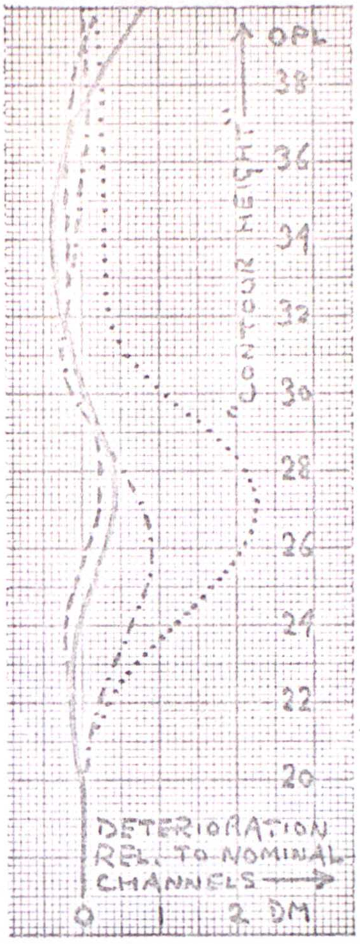

TROPICAL

FIG 2E

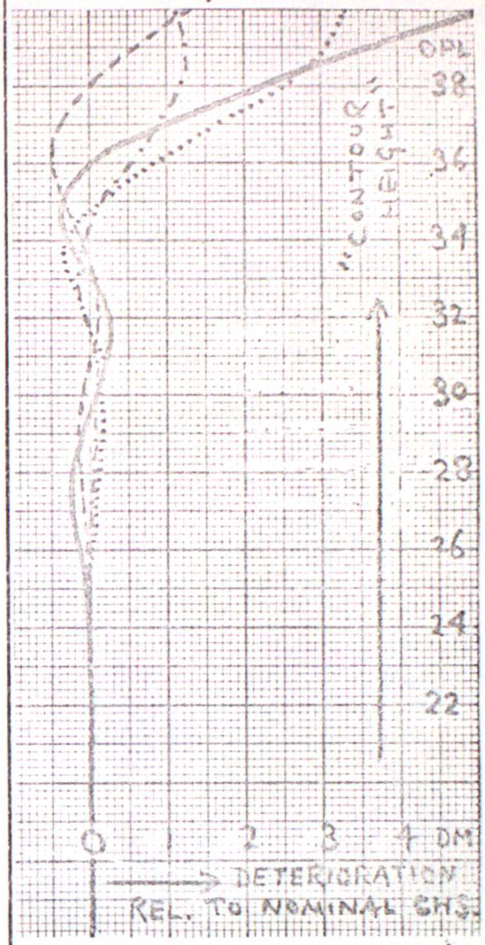

GAP A/B: WINTER 50/70

FIG 2C

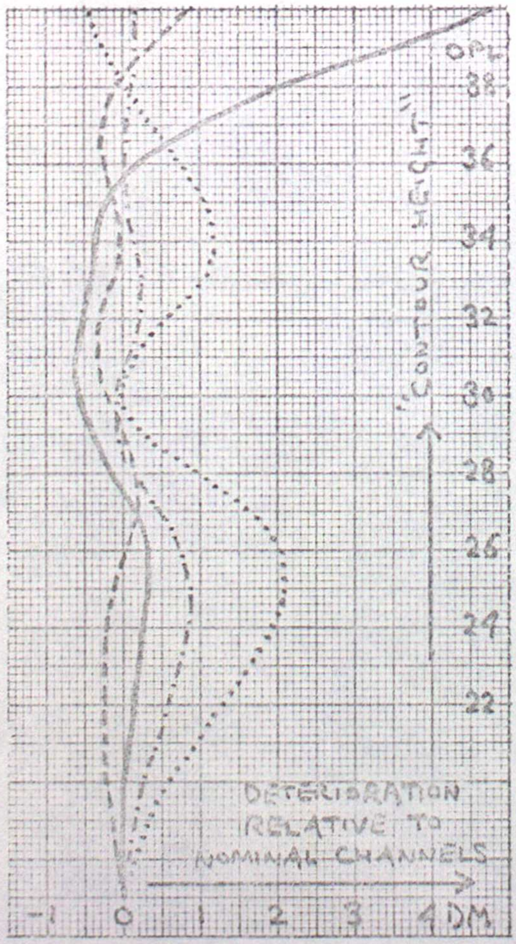

GAP B/C: WINTER 50 TO 70

FIG 2D

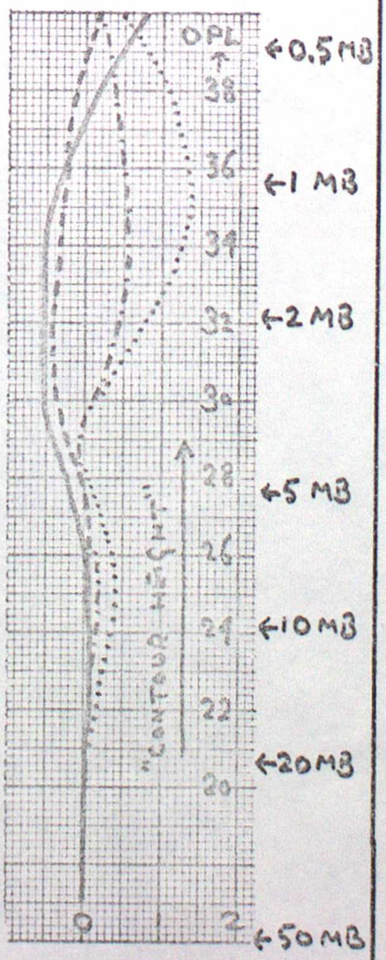

TROPICAL

KEY

GAP +4 LVLS

GAP +2 LVLS

GAP -2 LVLS

GAP -4 LVLS

KEY

FIG 2F

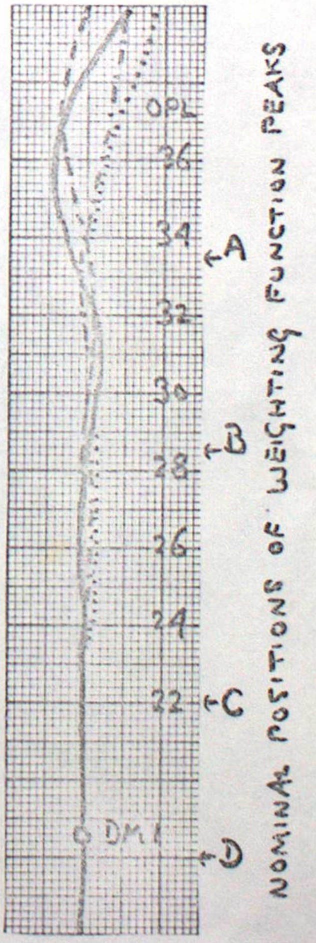

GAP A/B: TROPICAL

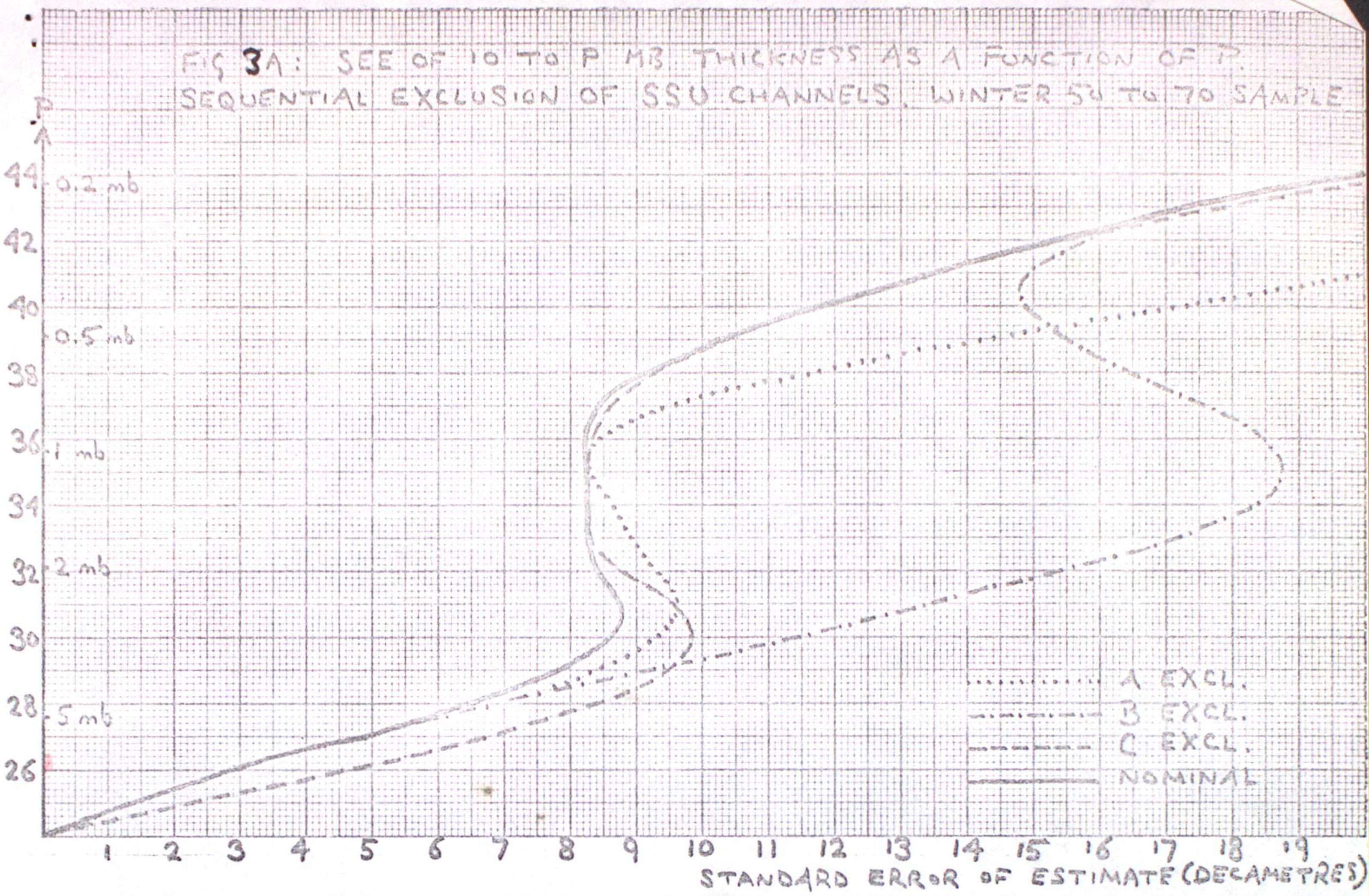
FIG 3A: SEE OF 10 TO P MB THICKNESS AS A FUNCTION OF P.
SEQUENTIAL EXCLUSION OF SSU CHANNELS, WINTER 50 TO 70 SAMPLE
P
0.2 mb
0.5 mb
1 mb
2 mb
5 mb
A EXCL.
B EXCL.
C EXCL.
NOMINAL
STANDARD ERROR OF ESTIMATE (DECAMETRES)

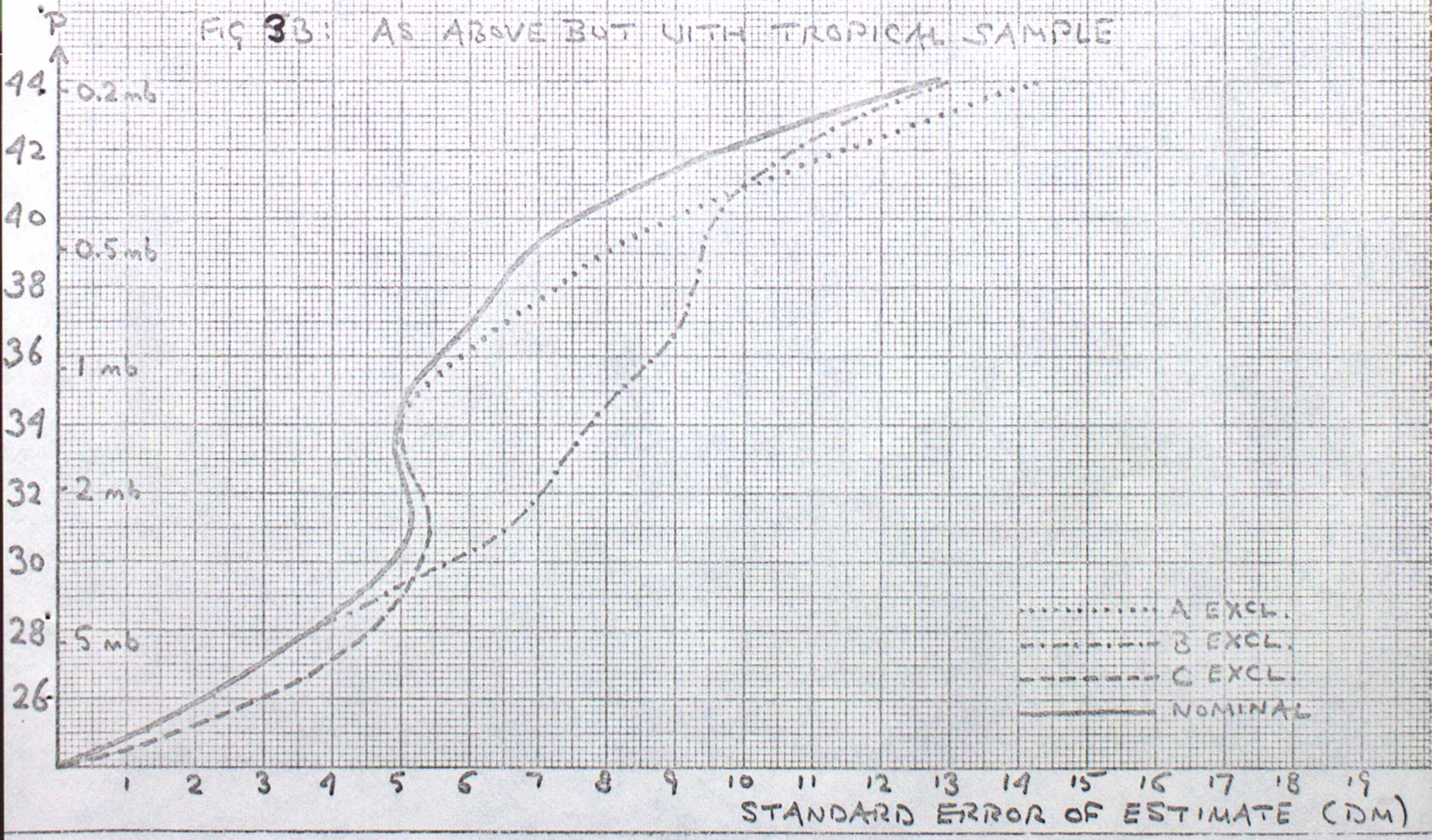
FIG 3B: AS ABOVE BUT WITH TROPICAL SAMPLE
P
0.2 mb
0.5 mb
1 mb
2 mb
5 mb
A EXCL.
B EXCL.
C EXCL.
NOMINAL
STANDARD ERROR OF ESTIMATE (DM)

"DETERIORATION IN "CONTOUR HEIGHT" S.E.E VALUES AS EACH INTER-CHANNEL SEPARATION IN TURN IS ALTERED.

BASE ≙ 10 MB (OXFORD PRESSURE LEVEL 24)

FIG 4A

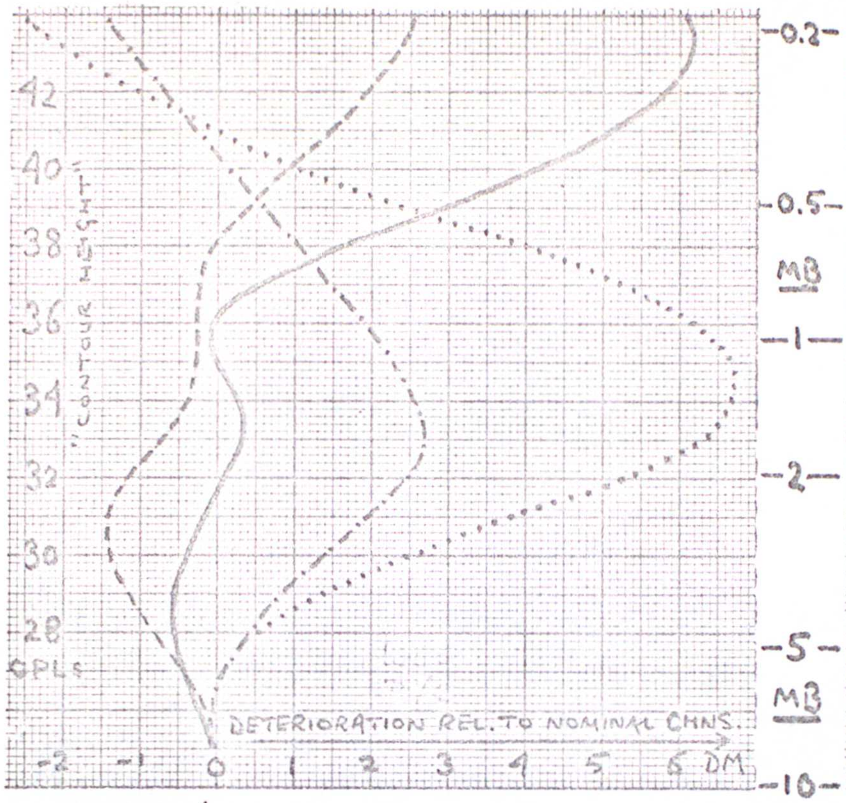

GAP B/C: WINTER 50 TO 70

FIG 4B

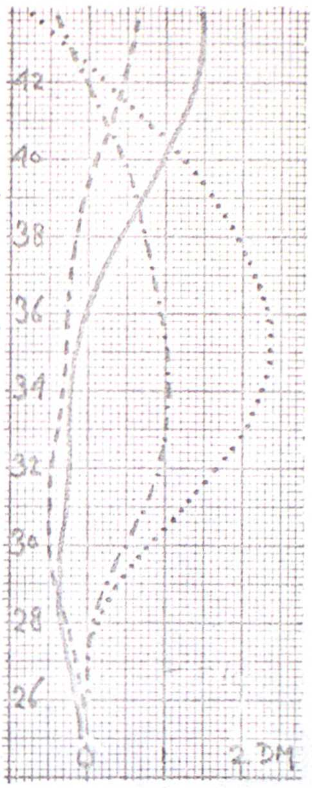

TROPICAL

FIG 4C

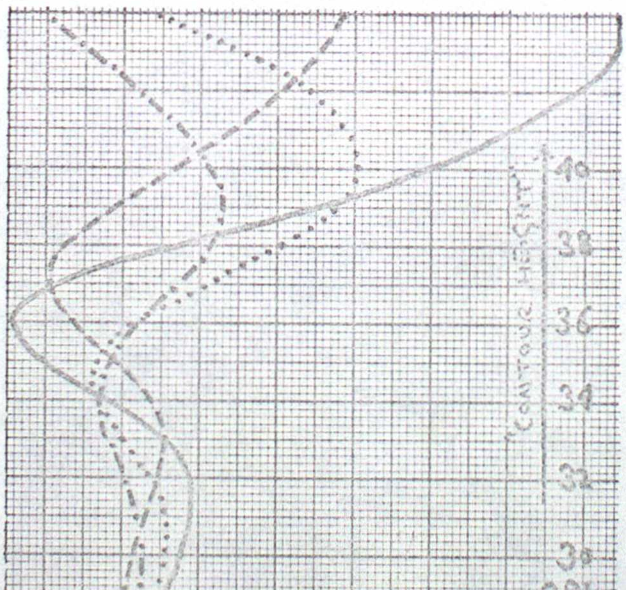

GAP A/B: WINTER 50-70

FIG 4D

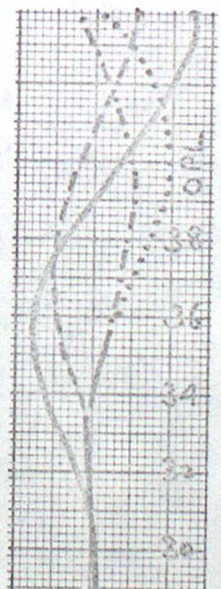

TROPICAL

NOMINAL POSITIONS:

C OPL 22
B OPL 28½
A OPL 33½

NOMINAL "GAPS"

B/C 6½ LEVELS
A/B 5 LEVELS

SEPARATIONS RELATIVE TO NOMINAL GAPS:

.... +4
-.-.-.-.-.- +2
------- -2
———— -4

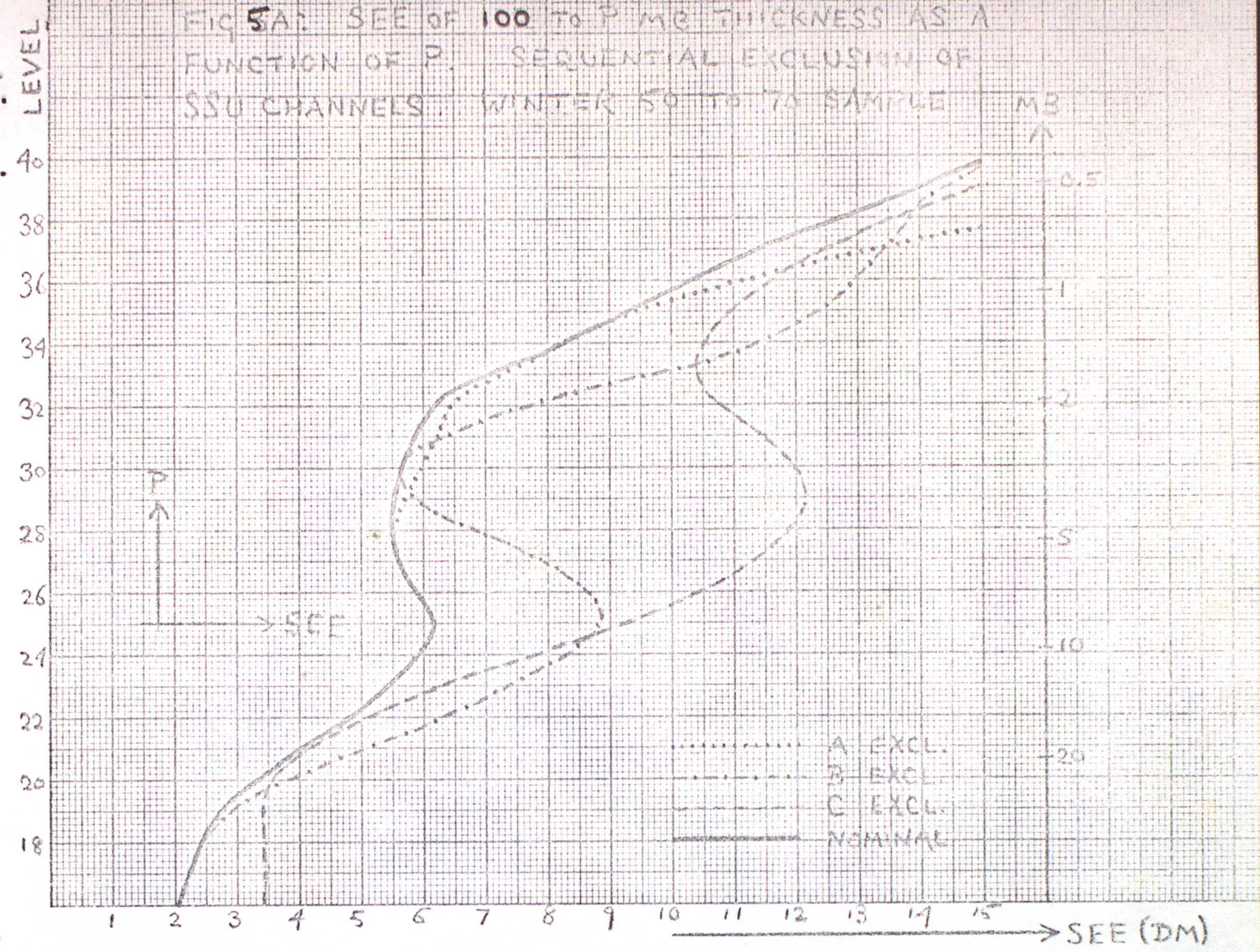

Fig 5A: SEE of 100 to P MB THICKNESS AS A FUNCTION OF P. SEQUENTIAL EXCLUSION OF SSU CHANNELS. WINTER 59 TO 73 SAMPLE

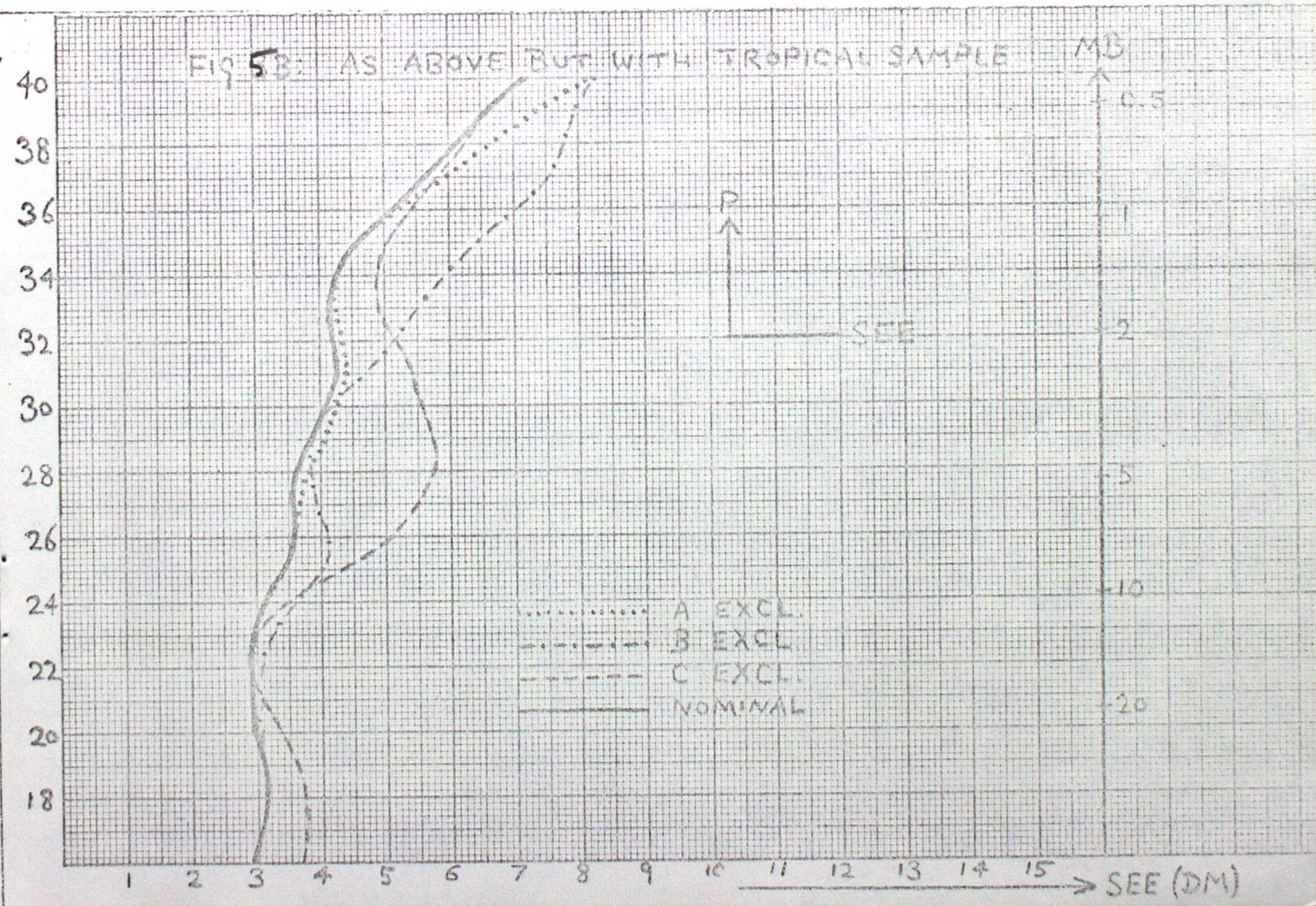

Fig 5B: AS ABOVE BUT WITH TROPICAL SAMPLE

APPENDIX

Derivation of Intermediate and Extrapolated Weighting Functions

OPL	WF
40	
39	
38	A+4
37	
36	
35	A+2
34	A
33	A-1
32	A-2
31	B+2
30	B+1
29	B
28	
27	B-2
26	
25	
24	C+2
23	
22	C
21	
20	C-2
19	
18	C-4

This table shows the positions (in terms of OPLs) of the peaks of the weighting functions used in the analysis. A, B and C represent the nominal weighting functions for the Tiros N SSU instrument. The A and B weighting function peaks are separated by 5 levels, while those corresponding to B and C are separated by $6\frac{1}{2}$ levels.

The shapes of the weighting functions are broadly though not exactly similar. Intermediate (and extrapolated) weighting functions are derived by "borrowing" the shape of the nearest nominal weighting function (A, B or C) and offsetting it by the appropriate number of levels. Errors arising out of this method are not thought to be serious at least as far as levels higher than level 16 (50.4mb) are concerned.

The table below shows the optimum weighting function to be used when one of the nominal WFs is required to be shifted by a given amount. The weighting function (B-$\frac{1}{2}$) was not available, so (B-2) approximates a +4 level shift of C.

Shift	A	B	C
+4	A+4	A-1	B-2
+2	A+2	B+2	C+2
0	A	B	C
-2	A-2	B-2	C-2
-4	B+1	C+2$\frac{1}{2}$	C-4

Noise

The distinctive property of the SSU is its sensitivity to temperature at high levels in the atmosphere. This is achieved by using in addition to conventional IR filters a set of pressure modulated cells (PMCs), cells containing CO_2 the pressure of which is modulated by an oscillating piston.

The measured SSU radiances are expected to contain random noise of rms value:

$$\frac{0.7}{\Delta W} \text{ radiance units}$$

$$1\ \mathrm{RU} = 1\ \mathrm{mW}(\mathrm{m}^2 .\ \mathrm{sr} .\ \mathrm{cm}^{-1})^{-1}$$

ΔW is the equivalent bandwidth of the appropriate PMC in wavenumbers per cm.

ΔW is roughly proportional to Δp_c, the amplitude of the pressure modulation. This in turn is related to the cell pressure p_c by the depth of modulation m.

The atmospheric pressure at the weighting function peak, p_o, is approximately proportional to p_c.

If m is constant, then

$$\Delta w \propto p_o$$

$$\text{rms noise} \propto 1/p_o$$

$$\text{noise variance} \propto 1/p_o^2$$

Thus the increase in noise variance due to a shift in a weighting function by Δn levels is given by

Increase in noise variance = $\exp(0.4\Delta n)$ *

This is a realistic approximation as far as channels A and B are concerned, and has been used to derive noise variance values for all "intermediate" weighting functions from (A+4) down to (B-2).

The modulation depth of the PMC corresponding to channel C is limited to 18% by the input power needed to drive the piston. The noise variance for channel C is only a small proportion of the radiance variance (0.2% for the winter 50-70° sample; 1.7% for the "worst case" tropical sample) and only a rough estimate for it is required. It has been assumed that for a downward shift (increase in cell pressure) the power input would be maintained so that m could be increased. In these circumstances, the effective bandwidth, and hence the noise variance, would not be expected to vary a great deal from its nominal value, and a figure of 0.12 RU^2 has been used for the noise variance of all "intermediate" weighting functions from (C+2½) down to (C-4).

The noise variances of BSU channels D and E are 0.20 and 0.03 RU^2 respectively.

Parameter	— CHANNEL — A	B	C	Units
Δw	0.4	1.0	2.0	cm^{-1}
rms noise	1.75	0.7	0.35	RU
noise variance	3.06	0.49	0.12	RU^2
p_o	1.5	4.0	15.0	mb (approx)
p_c	10	35	100	mb
m	30%	28%	18%	
Δp_c	3.0	9.9	18.3	mb

Nominal values of SSU parameters.

* Since the pressure at level n, $p_n = 1013.246 \exp -0.2(n-1)$ mb

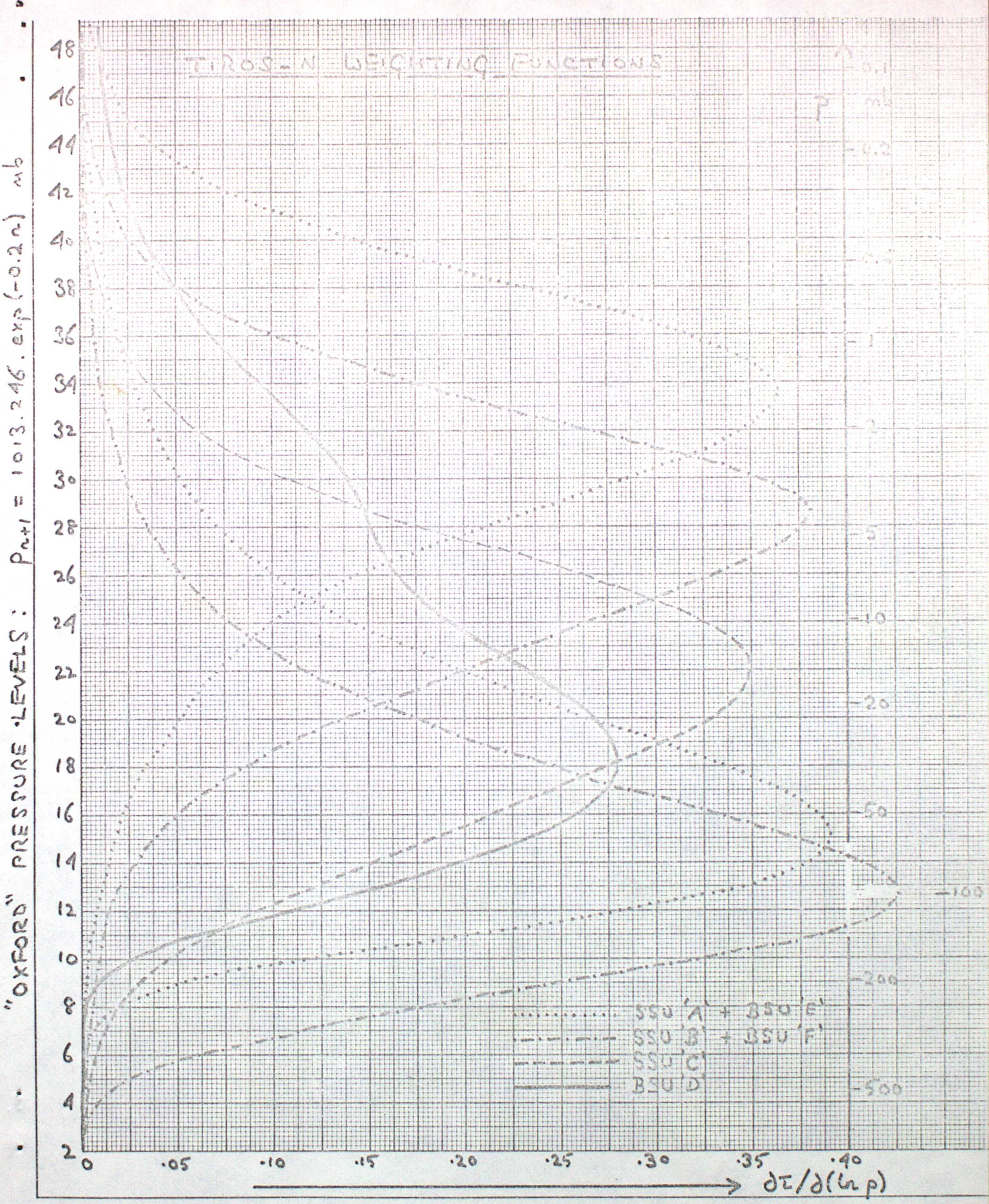
TIROS-N WEIGHTING FUNCTIONS
"OXFORD" PRESSURE LEVELS : $p_{n+1} = 1013.246 . \exp(-0.2n)$ mb
P
mb
0.1
0.2
0.5
1
2
5
10
20
50
100
200
500
48
46
44
42
40
38
36
34
32
30
28
26
24
22
20
18
16
14
12
10
8
6
4
2
0
·05
·10
·15
·20
·25
·30
·35
·40
SSU 'A' + BSU 'E'
SSU 'B' + BSU 'F'
SSU 'C'
BSU 'D'
$\partial\tau/\partial(\ln p)$

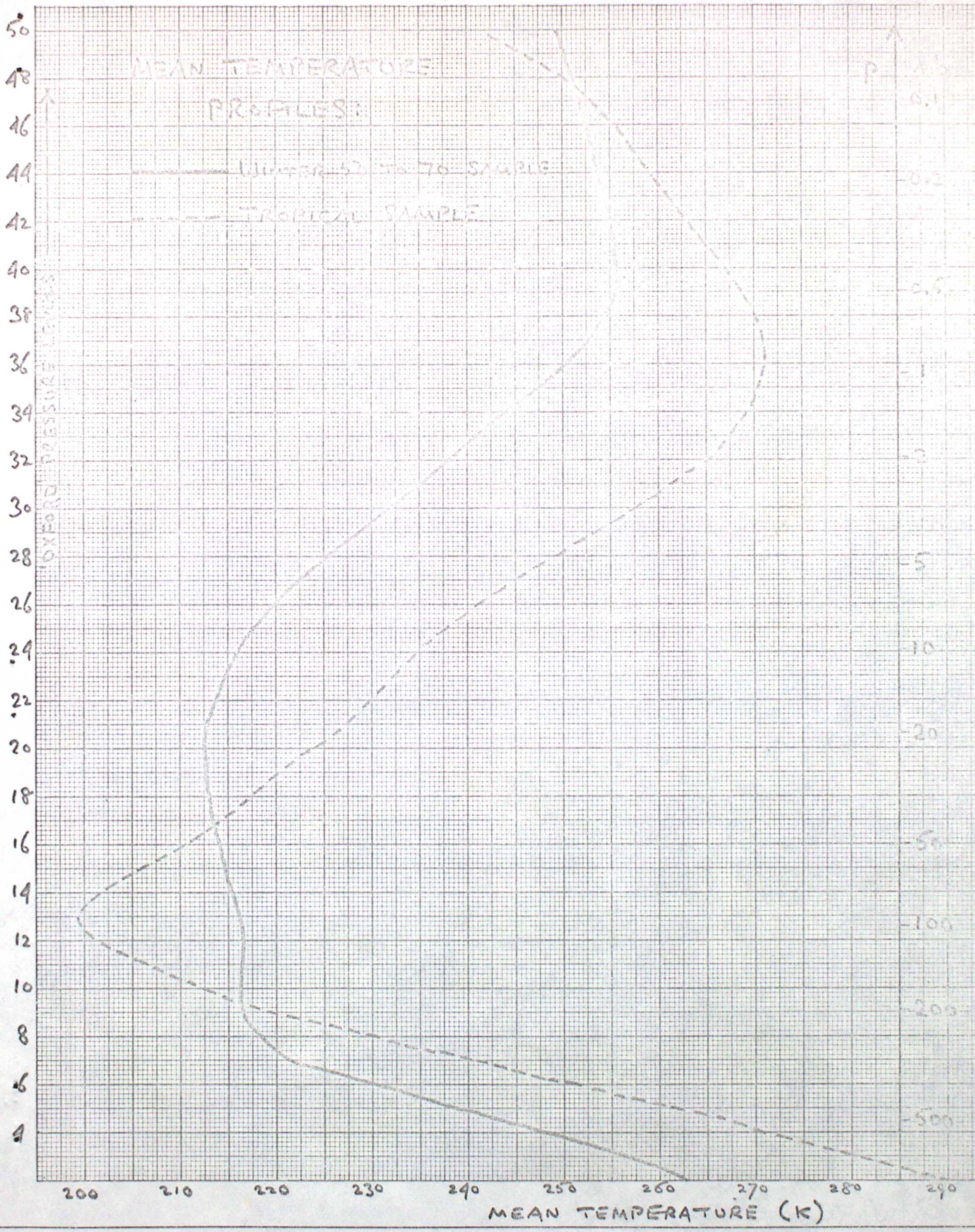
MEAN TEMPERATURE
PROFILES:
WINTER 60 TO 70 SAMPLE
TROPICAL SAMPLE
OXFORD PRESSURE LEVELS
50
48
46
44
42
40
38
36
34
32
30
28
26
24
22
20
18
16
14
12
10
8
6
4
P
0.1
0.2
0.5
1
2
5
10
20
50
100
200
500
200
210
220
230
240
250
260
270
280
290
MEAN TEMPERATURE (K)